



Review

# Recent Progress on PZT Based Piezoelectric Energy Harvesting Technologies

Min-Gyu Kang <sup>1,2</sup>, Woo-Suk Jung <sup>3</sup>, Chong-Yun Kang <sup>1,4</sup> and Seok-Jin Yoon <sup>1,\*</sup>

<sup>1</sup> Electronic Materials Research Center, Korea Institute of Science and Technology, 39-1 Hawolgok-Dong, Sungbuk-gu, Seoul 136-791, Korea; jws7216@gmail.com (W.-S.J.); cykang@kist.re.kr (C.-Y.K.)

<sup>2</sup> Bio-inspired Materials and Devices Laboratory (BMDL), Center for Energy Harvesting Materials and Systems (CEHMS), Virginia Tech, Blacksburg, VA 24061, USA; mgkang@vt.edu

<sup>3</sup> Department of Digital Electronics, Daelim University College, 29 Imgoklo Dongan-gu, Anyang-si, Gyunggi-do 431-715, Korea

<sup>4</sup> KU-KIST Graduate School of Converging Science and Technology, Korea University, Seoul 136-701, Korea

\* Correspondence: sjyoon@kist.re.kr; Tel.: +82-2-958-5550 (ext. 123); Fax: +82-2-958-6720

Academic Editor: Kenji Uchino

Received: 3 December 2015; Accepted: 1 February 2016; Published: 22 February 2016

**Abstract:** Energy harvesting is the most effective way to respond to the energy shortage and to produce sustainable power sources from the surrounding environment. The energy harvesting technology enables scavenging electrical energy from wasted energy sources, which always exist everywhere, such as in heat, fluids, vibrations, *etc.* In particular, piezoelectric energy harvesting, which uses a direct energy conversion from vibrations and mechanical deformation to the electrical energy, is a promising technique to supply power sources in unattended electronic devices, wireless sensor nodes, micro-electronic devices, *etc.*, since it has higher energy conversion efficiency and a simple structure. Up to now, various technologies, such as advanced materials, micro- and macro-mechanics, and electric circuit design, have been investigated and emerged to improve performance and conversion efficiency of the piezoelectric energy harvesters. In this paper, we focus on recent progress of piezoelectric energy harvesting technologies based on  $\text{PbZr}_x\text{Ti}_{1-x}\text{O}_3$  (PZT) materials, which have the most outstanding piezoelectric properties. The advanced piezoelectric energy harvesting technologies included materials, fabrications, unique designs, and properties are introduced to understand current technical levels and suggest the future directions of piezoelectric energy harvesting.

**Keywords:** PZT; energy harvesting; piezoelectric

## 1. Introduction

Energy harvesting, which collects useful energy from wasted energy sources, is the most promising technology to provide solutions for the shortage of a fossil fuel, various environmental problems, and the improvement of energy efficiency in smart grids. The basic concept of energy harvesting technology is to obtain the electrical energy by an energy conversion from a wasted heat, a vibration, a mechanical deformation, a potential energy, *etc.* The driving force for the piezoelectric energy harvesting is also the energy conversion effect using piezoelectricity. Up to now, the piezoelectric effect, which is an energy conversion phenomena leading to the electrical energy generated by an applied force and a mechanical deformation by an applied electric field, have been extensively utilized to demonstrate various devices, such as transducers [1,2], sensors [3–5], actuators [6,7], surface acoustic wave (SAW) devices [8,9], frequency control, *etc.* [10]. In the past decade, piezoelectric energy harvesting technologies have been intensively investigated in various research

fields, such as material science, electrical engineering, mechanical engineering, bio-medical science, *etc.*, since it has the remarkable energy conversion efficiency. The piezoelectric energy harvesting technologies can be utilized for the self-power sources in battery-less devices operated by small power at the mW-μW level, and power sources in portable systems, wireless sensor systems, health monitoring systems, and the military and vehicle industry [10,11]. Recently, the piezoelectric energy harvesters with unique structures and fabrication methods have been significantly developed, which can be classified with bulk type, microelectromechanical systems (MEMS), and flexible energy harvesters.

The piezoelectric materials, which contain dense polycrystalline and single crystalline ceramics have been investigated for achieving high piezoelectric charge constant ( $d$ ), voltage constant ( $g$ ), electromechanical coupling factor ( $k$ ), and mechanical quality factor ( $Q_m$ ), which are figures of merit (FOM) of the piezoelectric materials for the energy harvesting. Each factor is expressed as the following [12],

1. Piezoelectric strain (unit: pm/V) and charge (unit: pC/N) constant

$$x = dE \quad (d = \text{piezoelectric strain and charge constant}) \quad (1)$$

where  $x$  and  $E$  are strain and external electric field.

2. Piezoelectric voltage constant (unit: Vm/N)

$$E = gX \quad (g = d/\epsilon_0\epsilon_r) \quad < g = \text{piezoelectric voltage constant} > \quad (2)$$

where  $\epsilon_0$  and  $\epsilon_r$  are dielectric constant in a vacuum and relative dielectric constant.

3. Electromechanical coupling factor

$$k^2 = (\text{Stored mechanical energy}/\text{Input electrical energy}) \quad (3)$$

$$k^2 = (\text{Stored electrical energy}/\text{Input mechanical energy}) \quad (4)$$

Since the input electrical energy is  $(1/2)\epsilon_0\epsilon_r E^2$  per unit volume and the stored mechanical energy per unit volume under zero external stress is given by  $(1/2)x^2/s = (1/2)(dE)^2/s$ ,  $k^2$  can be calculated as

$$k^2 = [(1/2)(dE)^2/s]/[(1/2)\epsilon_0\epsilon_r E^2] = d^2/\epsilon_0\epsilon_r s \quad (5)$$

where  $s$  is stress.

4. Mechanical quality factor

$$Q_m = \omega_0/2\Delta\omega \quad (6)$$

where  $\omega_0$  is resonance frequency.

The piezoelectric material with higher  $d \times g$  (transduction coefficient) and higher  $g$  value especially provides higher output electrical power. Hence, the  $d$  and  $g$  values are the essential criteria for the piezoelectric materials used for energy harvesting applications.

The piezoelectric thin films are also used in a variety of applications in the microelectronics industry for example in sensors and MEMS piezoelectric energy harvesting for a micro electricity generation. The effective piezoelectric constants  $d$  and  $e$  values are usually used as FOM factors for the thin film materials. Conventionally, the  $d_{33,f}$ , effective piezoelectric strain constant, has been determined by a piezoelectric force microscopy (PFM) technique. The electric field induced the surface deflection on the thin film piezoelectric material is measured by an atomic force microscopy (AFM) with a conductive cantilever tip and the  $d_{33,f}$  value can be calculated from the displacement divided by a applied voltage (unit: pm/V). The effective piezoelectric constant  $e_{31,f}$  is defined as  $e_{31,f} = d_{31}/(s_{11}^E + s_{12}^E)$  (unit: C/m<sup>2</sup>) [13]. Where  $d_{31}$  is the in-plane piezoelectric constant and  $s_{11}^E + s_{12}^E$  are the in-plane elastic compliances of the bulk material. The  $e_{31,f}$  value has been evaluated by a wafer flexure method [14]. The wafer flexure method depends on the pressurization or evacuation

of a cavity to which a simply supported wafer is sealed. During this stress oscillation, a charge integrator is connected to the sample, which measures the piezoelectric charge, and allows calculation of the stress-induced polarization.

Since large piezoelectric coefficients in  $\text{PbZr}_x\text{Ti}_{1-x}\text{O}_3$  (PZT) solid solution systems were discovered, the various composition of PZT based piezoelectric materials have been studied to obtain a higher piezoelectric coefficient ( $d_{33} = \sim 300\text{--}1000$  pC/N) [15] and also alternate materials have been discovered to achieve the lead-free piezoelectric materials.  $\text{Na}_x\text{K}_{1-x}\text{NbO}_3$  (NKN) piezoelectric ceramics are suggested for one of the promising alternate materials of the PZT, which includes non-toxic and environmental friendly materials with high piezoelectric coefficient ( $d_{33} = \sim 100\text{--}400$  pC/N) [16,17]. However, the piezoelectric performance as the piezoelectric coefficient and the electromechanical coupling is still much lower than the PZT based materials. A piezoelectric AlN thin film is also attractive for the MEMS piezoelectric energy harvesting, because it can be obtained by a reactive sputtering method easily and has a low dielectric permittivity leading to high piezoelectric voltage coefficient. Nevertheless, the piezoelectric coefficient is still very small compared to the PZT based materials ( $d_{33} = \sim 3\text{--}5$  pm/V) [18]. Since Wang *et al.* discovered a coupling of the piezoelectric and the semiconducting properties in single crystalline ZnO nanowires ( $d_{33} = \sim 14\text{--}26$  pm/V) [19], the nano-structured ZnO materials have been studied as an attractive material for the piezoelectric energy harvesting [20]. The ZnO thin films and nanostructured materials are easily synthesized at low process temperature and can be integrated on flexible organic substrates for future flexible, stretchable, and portable electronics [21]. Moreover, the low dielectric permittivity of the ZnO materials improves the output performance of the piezoelectric energy harvesters. Despite of remarkable advantages in ZnO materials, the PZT based materials still have been considered as the most outstanding piezoelectric materials for the energy harvesting due to their much higher piezoelectric coefficients.

In this paper, we have reviewed recent progress on the PZT based piezoelectric materials and the devices for the energy harvesting. In recent years, a large amount of the considerable technical approaches regarding the PZT based piezoelectric energy harvesting have been reported. The piezoelectric material included bulks, thin films, and nanostructured materials with various composition and morphologies, and unique designs to improve the energy conversion efficiency of the piezoelectric energy harvesting, and desirable applications using bulk type, MEMS, and flexible piezoelectric harvesters have been suggested.

## 2. Bulk Type Piezoelectric Energy Harvesters

Various structural designs and material compositions for the bulk type piezoelectric energy harvesters have been investigated to improve the conversion efficiency for the various applications. The operating performance of the energy harvesters is strongly affected by acceleration, applied force, vibration frequency, impedance matching, mass, and surrounding environment, structural design and materials. In this section, various design of bulk type piezoelectric energy harvesters are introduced including cantilever type, cymbal type and stack type energy harvesters for self-powered devices, water flow sensors, tire pressure monitoring system, *etc.*

### 2.1. Cantilever Type Piezoelectric Energy Harvesters

A cantilever type piezoelectric harvester is one of the promising structures to obtain high output power from the piezoelectric element, because it can apply larger strain to the piezoelectric elements under vibration condition. A general structure of the cantilever type piezoelectric energy harvester is illustrated in Figure 1a. The harvester consists of the piezoelectric ceramic, elastic body, and proof mass. This simple structure produces a large deformation under a vibration environment and can effectively collect the electrical power from the piezoelectric ceramic in 31 mode. Each physical factor in the devices (length, area, mass, thickness and position of the piezoelectric ceramics and elastic body, *etc.*) determines the operating performance of the harvester. To evaluate the performance of the cantilever type piezoelectric harvester, conventionally, such an experimental setup has been used as

shown in Figure 1b. A function generator and an amplifier are used to operate an exciter with various frequencies and accelerations, and an electric circuit containing loads, capacitors, and a rectifier is connected with the harvester for an impedance matching and rectifying of the output signal. The volumetric output power ( $\text{W}/\text{cm}^3$ ) is usually used to present the performance for the harvester and can be calculated from the generated voltage and the current value. The output power tends to be tuned by depending on the load resistance, the acceleration level, and the frequency of the vibration. Therefore, these factors should be optimized to obtain a maximum power output from the piezoelectric energy harvesters.

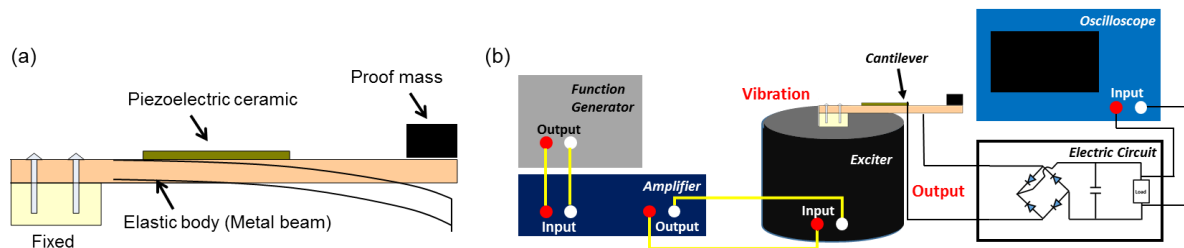


**Figure 1.** (a) Schematic of cantilever type piezoelectric energy harvester; (b) conventional experimental setup to evaluate cantilever type piezoelectric energy harvester.

Various research groups have investigated the simple cantilever and modified cantilever type piezoelectric harvesters. To enhance the output performance of the piezoelectric energy harvester, the material properties are the most important factor. Kim *et al.* demonstrated a unimorph cantilever type piezoelectric energy harvester using modified PZT thick films. Cr and Nb co-doping in the PZT ceramics improved  $d_{33} \cdot g_{33}$  value up to  $14,072 \times 10^{-15} \text{ m}^2/\text{N}$ , which is an FOM for the piezoelectric energy harvesting. From this, they obtained the maximum electrical power of 17.3 mW ( $2.08 \text{ mW}/\text{cm}^3$ ) at 20 Hz under  $\sim 4 \text{ g}$  ( $g = 9.8 \text{ m}/\text{s}^2$ ) [22]. Choi *et al.* investigated a relationship between the piezoelectric properties and the output power of the piezoelectric energy harvester. They used the modified PZT ceramics with  $\text{Pb}[(\text{Zn}_{0.4}\text{Ni}_{0.6})_{1/3}\text{Nb}_{2/3}]\text{O}_3$  (PZNN) in addition to exploring an optimum composition leading to the maximum piezoelectric properties. They revealed that the output power of the piezoelectric energy harvesters are linearly increased with increasing the  $d_{33} \cdot g_{33}$  value and obtained the maximum electrical power of  $231 \text{ mW}/\text{cm}^3$  from the piezoelectric cantilever at 84 Hz under 1 g [23]. Normally, the piezoelectric properties of the PZT based ceramics tend to be degraded at high temperature. Kim *et al.* studied the temperature dependent output power of the bimorph piezoelectric energy harvester with soft and hard PZT materials. Both cantilevers exhibited degraded output power in a high temperature range ( $50^\circ\text{C} < T < 150^\circ\text{C}$ ) resulting from the sharply raised dielectric permittivity [24].

Generally, single crystal piezoelectric materials have significantly improved piezoelectric properties compared to the polycrystalline ceramics. Song *et al.* investigated the performance of the cantilever type piezoelectric energy harvesters using three different types of the piezoelectric materials including  $0.7\text{Pb}(\text{Mg}_{1/2}\text{Nb}_{2/3})\text{O}_3\text{-}0.3\text{PbTiO}_3$  (PMN-PT) single crystals oriented along the  $\langle 110 \rangle$  and  $\langle 001 \rangle$  directions, and the PZT based polycrystalline ceramics [25]. The piezoelectric energy harvester with  $\langle 110 \rangle$  oriented PMN-PT single crystal maximized the electrical power output among them. The maximum power was 1.07 mW at 89 Hz under 0.53 g. The cantilever type piezoelectric energy harvester was operated in 31 mode and the  $\langle 110 \rangle$  oriented PMN-PT single crystal exhibited the maximized electromechanical coupling factor in the 31 mode. Karami *et al.* compared the piezoelectric performance of the unimorph cantilever type energy harvesters with single crystal PMN-PZT and the commercial PZT based materials, such as PZT-5A and PZT-5H. They revealed that the single crystal piezoelectric energy harvester produces superior power output compared to the polycrystalline piezoelectric ceramics. The maximum output from the cantilever was  $226 \mu\text{W}/\text{g}^2$  at 819 Hz [26].

To maximize the output power of the piezoelectric energy harvester, the cantilever type piezoelectric energy harvesters have been usually operated in a mechanical resonance frequency (natural frequency). Therefore, tuning of the natural frequency of the piezoelectric energy harvester is important to determine applications. The undamped natural frequency of the cantilever in a transverse vibration is given by

$$\omega_0 = \sqrt{\frac{k_{eq}}{m_{eq}}} = \sqrt{\frac{3YI/L^3}{(33/140)mL + M_t}} \quad (7)$$

where  $k_{eq}$  is the equivalent spring rate,  $m_{eq}$  is the equivalent mass,  $YI$  is the flexural rigidity of the beam,  $L$  is the length of the beam,  $m$  is the mass per unit length, and  $M_t$  is the tip mass,  $33/140$  mean that  $33/140$  (23.5%) of the beam mass participate in the motion. From Equation (7), it can be known that the natural frequency is tuned by changing the spring constant, mass, beam length, width, and thickness of the cantilever [27]. To modify natural frequency of the piezoelectric energy harvester, Berdy *et al.* demonstrated the piezoelectric energy harvester using a meandering structure. The meandering structure, which leads to increase of the body length, resulted in reducing the natural frequency of the cantilever, and the output power was 118  $\mu$ W at 49.7 Hz of natural frequency under 0.2 g [28]. Shindo *et al.* also achieved the low natural frequency using a S-shape cantilever structure with the output power of 8.5 mW/cm<sup>3</sup> at 40 Hz under 3.2 g [29]. A wide bandwidth of the natural frequency enhances the capability of the piezoelectric energy harvesters for the various applications. Sobocinski *et al.* firstly introduced the fully embedded wideband piezoelectric energy harvester using a low temperature co-fired ceramic (LTCC) technique. They realized an integrated system including a reliable and hermetic package, a circuit board for electronics and three kinds of active piezoelectric harvester structures in the same process. Three cantilevers with different lengths had a variety of natural frequencies and exhibited 5.4% frequency bandwidth for 3 dB attenuation. The maximum power output was 32  $\mu$ W at 1100~1165 Hz under 1 g acceleration [30]. From these results, it is clear that control of the natural frequency can be easily achieved by the tuning length of the cantilever. The low and wide resonance frequency of the cantilever expands the application field in the environmental vibration conditions. The output performance of the bulk cantilever energy harvesters is summarized in Table 1.

**Table 1.** Comparison of the output performance of the cantilever type bulk piezoelectric energy harvesters.

Structure	Power Density (mW/cm <sup>3</sup> )	Normalized Power (mW/g <sup>2</sup> )	Frequency (Hz)	Ref.
Cr and Nb doped PZT cantilever	2.1	1.1	20	[22]
PZNN cantilever	231	11.7	84	[23]
<110> oriented single crystalline PMN-PT cantilever	-	3.8	84	[25]
<001> oriented single crystalline PMN-PT cantilever	-	1.4	86	[25]
PMN-PZT single crystalline cantilever	-	0.2	819	[26]
Meandering structured cantilever	0.2	2.9	50	[28]
S-shape bulk cantilever	8.5	-	40	[29]
Wideband LTCC cantilever arrays	-	0.03	1100–1165	[30]

The cantilever type energy harvesters have been usually designated for operating under simple vertical vibration conditions. However, the environmental vibrations and the mechanical energy sources around it are actually not simple. Here, we introduce new challenges on the cantilever type energy harvesters for special applications without the simple vertical vibration. They determined the optimal structural design of the piezoelectric energy harvesters according to the various mechanical energy sources. Park *et al.* investigated bimorph piezoelectric energy harvesters with an asymmetric



inertial mass for a multi-dimensional vibration ambient. The asymmetric inertial mass contributes to generating power from the vibration applied to the length and thickness directions of the PZT cantilever. They obtained the output power of 7.5 mW for the z-axis and 1.4 mW for the x-axis at 45 Hz under 1 g [31]. The multi-dimensional vibration energy harvester is an effective device to generate electrical power from the vibration of a vehicle. Hashimoto *et al.* demonstrated a multi-mode and multi-axis piezoelectric energy harvester using a two-mass device with two bending modes for the vehicle application. They performed a road test using the prototype energy harvester and acquired a high energy efficiency from the device [32]. For the multi-axis piezoelectric vibration energy harvesting, Erkan *et al.* fabricated a crab-leg like cantilever structure via individually assembling processed bulk-PZT leg on a patterns silicon die. They obtained 5–50  $\mu$ W power at 387–389 Hz under 50 mg acceleration amplitude in the *x*, *y*, and *z* direction from the multi-axis piezoelectric energy harvester [33]. Khameneifar *et al.* proposed a rotary type piezoelectric energy harvester using four cantilever type harvesters. In this structure, mechanical vibration energy is applied on the PZT cantilevers due to a gravitational force while the hub is rotating. They obtained maximum power of 6.4 mW at a shaft speed of 138 rad/s [34]. This rotary type energy harvester is also useful for the wind energy harvesting using impact-induced resonance operation [35]. The off-resonance operation with the high power output of the piezoelectric energy harvester can achieve more practical ways to use the various applications around it. For this, Pozzi *et al.* demonstrated a prototype piezoelectric energy harvester with four PZT bimorph cantilevers that is wearable on knee joints. The energy harvester relies on the plucking technique, and the PZT cantilevers are deflected by a plectrum; when released due to loss of a contact, the cantilevers are free to vibrate at their resonant frequency. The average power output of the prototype harvester reached 2.06 mW [36]. Li *et al.* presented a low frequency acoustic energy harvester using a PZT cantilever. The acoustic piezoelectric energy harvester contained a quarter-wavelength straight tube resonator with the PZT piezoelectric cantilever placed inside the tube. The maximum output power of 12.697 mW was generated in an incident sound pressure of 110 dB [37].

## 2.2. Various Types of Bulk Piezoelectric Energy Harvesters

Unique structures of the bulk type piezoelectric harvesters have been proposed for the various applications. Palosaari *et al.* demonstrated cymbal type piezoelectric energy harvester. A piezoelectric disc was confined between two convex steel discs acting as a force amplifier delivering stress to the PZT discs and protecting the harvester. At 1.19 Hz compression frequency with 24.8 N force, a cymbal type harvester generated an average power of 0.66 mW and the maximum power densities of 0.31 mW/cm<sup>3</sup> were observed [38]. Chen *et al.* introduced a piezoelectric energy harvester with a clamped piezoelectric circular diaphragm structure, which is a common structure for pressure sensors. The electrical power of 12 mW was obtained when a pre-stress of 1.2 N was applied on the harvester at 113 Hz under 1 g [39]. Multilayer stack structure for an energy harvesting using 33 mode achieved enhancing of the mechanical to the electrical energy conversion efficiency [40,41]. Xu *et al.* obtained significantly higher electrical power than a similar size cantilever type piezoelectric energy harvester in both resonance and off-resonance modes. The generated electrical powers were 2 mW at 700 Hz (off-resonance) and 208 mW at 1714 Hz (resonance) [41]. The piezoelectric energy harvester can be utilized for battery- and wire-less tire pressure measurement systems (TPMS). Makki *et al.* embedded the stacked piezoelectric bender elements in a tire wheel for an in-wheel based power harvesting [42]. This utilizes the cyclic deformation of the tire during vehicle movement. The weight of the vehicle deforms the tire at the tire-road interface created on the piezoelectric sensors. As the tire rotates during vehicle movements, a new section of the tire's treadwall deforms within the piezoelectric sensors resulting in a cyclic deformation and relaxation pattern.

### 3. MEMS Piezoelectric Energy Harvesters

Decreasing flexural rigidity associated with the piezoelectric energy harvesters is very attractive to reduce the natural frequency and withstand large strain and deformation. The MEMS technology is one of the promising choices to utilize the low flexural rigidity of the piezoelectric energy harvesting devices. Moreover, tiny piezoelectric devices fabricated by the MEMS process can be easily integrated in the micro-electronics that require the power source of  $\mu\text{W}$  level [43–45]. Generally, the structure of the MEMS piezoelectric harvesters based on the cantilever structure have been mainly developed to obtain the high output power and easily enable tuning the resonance frequency [46–49]. The general MEM cantilever structure is similar to the bulk energy harvester [50]. The Si or metal is used for the elastic body, the piezoelectric film is the active piezoelectric materials, and the proof mass is formed to tune the resonance frequency and the applied force. Modified cantilever structure [51], diaphragm structure [52], *etc.* have also been suggested for the high efficiency and practical applications.

In this section, we introduce various structural designs and properties of the MEMS energy harvesters. Kim *et al.* demonstrated a bimorph PZT cantilever for energy harvesting application. They compared the piezoelectric properties under  $d_{31}$  unimorph,  $d_{31}$  bimorph,  $d_{33}$  unimorph, and  $d_{33}$  bimorph modes. At the resonance of 89.4 Hz, they obtained the maximum average power about 3.9 ( $d_{31}$  unimorph), 9.6 ( $d_{31}$  bimorph), 9.6 ( $d_{31}$  bimorph), 21.42 ( $d_{33}$  unimorph), and 22.47 ( $d_{33}$  bimorph) nW under 0.8 g, respectively [53]. To compare the output power of the  $d_{31}$  and  $d_{33}$  mode MEMS cantilevers, Kim *et al.* demonstrated both types of the energy harvesters with the same dimension in a cantilever structure leading to the same resonance frequency at 243 Hz. The results of modeling and experiment studies obtained almost the same output power. From the experiments, they obtained a slightly higher output performance from the  $d_{33}$  mode cantilever. Although the harvester with  $d_{33}$  mode showed higher output performances, however, they have mentioned that the electrode design of  $d_{33}$  mode should be conducted carefully, because the output power strongly depends on the dimensions of inter digital electrode (IDE) [54]. These results indicate that the output power of the MEMS cantilever is strongly affected by an electrode configuration and poling direction of the piezoelectric materials. To increase output power and energy conversion efficiency, Tang *et al.* fabricated a PZT microstructure using bulk ceramics [55]. Through the previous research, they obtained the optimized shape of the cantilever beam and mass, which was determined through simulations and experimental study, resulting in the output voltage of  $\sim 1$  V at the resonance frequency around 1 kHz [56]. They used patterning on bulk ceramics by a dicing to demonstrate the rectangular micro-poles. The fabricated micro-cantilevers, which have different lengths and masses, and the resonance frequency around 520 Hz, were assembled on a printed circuit board (PCB). The output power and voltage were varied with the different frequency, acceleration, and load. The maximum output power was  $\sim 28.8$  mW/cm<sup>3</sup> at the resonance frequency with load of 70 k $\Omega$  under 1 g of acceleration. Kuehne *et al.* presented a novel MEMS generator for fluid-actuated energy conversion [51]. They fabricated a narrow fluidic cantilever tip to increase an energy conversion efficiency. In the experimental study, the electrical quality factors and energy density of rectangular and triangular cantilevers were compared under the various ambient pressures and cantilever deflection of the free-end. The compared electrical energy density value of the rectangular shape was three times larger. The maximum energy density value for the triangular cantilever shape was measured to 35 nJ/mm<sup>2</sup>.

A metal-based MEMS cantilever is a promising structure to get the flexibility to reduce the resonance frequency and enhance a strain. Wang *et al.* demonstrated the metal-based MEMS cantilever. The PZT thick film was deposited on the stainless steel beam by a sol-gel method, which has approximately 4  $\mu\text{m}$  thickness. Around 90 Hz, the cantilever has the resonance frequency, and the maximum output power was 15  $\mu\text{W}$  under 89 Hz and 1 g acceleration [57]. Lin *et al.* fabricated a piezoelectric micro energy harvester using a high-quality PZT thick film on stainless steel that was deposited by an aerosol deposition method. It generated the maximum output power of 200.28  $\mu\text{W}$  with a 12.67 V<sub>p-p</sub> output voltage at 112.4 Hz under 1.5 g acceleration and the energy densities of the device in a vacuum and in atmosphere were calculated as 178.6 and 137.5 nJ/mm<sup>3</sup>, respectively [58].

Normally, the conventional MEMS cantilever has been operated at a high frequency ( $>1$  kHz), because of short length and small mass of the cantilever beam. Furthermore, the amplitude bandwidth at the resonance frequency is very narrow. However, ambient vibration sources around usually have a wide bandwidth and low frequency, normally less than 200 Hz. In the MEMS piezoelectric harvesting technology, achieving low resonance frequency and wide frequency range operation is the most important goal for the practical application. The tuning configuration of the mass on the cantilever is a general method to achieve low resonance frequency. Liu *et al.* demonstrated the piezoelectric MEMS energy harvester with a wideband operation range and steadily increased output power. The resonance frequency of the fabricated MEMS generator had around 36 Hz due to the Si mass configuration. To achieve the wide bandwidth, they also embedded the cantilever arrays with different PZT elements and limited spacers, which is a common technique to acquire the wide bandwidth. The whole chip was assembled onto a metal carrier with the limited spacer such that the operation frequency bandwidth can be widened to 17 Hz at the input acceleration of 1.0 g during frequency up-sweep. Load voltage and power generation for the different numbers of the PZT elements in series and in parallel connections were compared and discussed in this paper. Under the same input acceleration, the optimal power was the same. However, the impedance measured at the maximum output power was reduced by connecting PZT elements in parallel. The electrical power generated at 1.0 g with respect to the load resistance of 330 k $\Omega$  achieved a wideband output ranging from 32.3 nW to 85.5 nW within the operation bandwidth from 30 Hz to 47 Hz [59,60]. They also fabricated a new S-shaped MEMS PZT cantilever with a low frequency vibration. The long length of the S-shape cantilever beam effectively reduced the resonance frequency of the device. The S-shaped MEMS cantilever could be operated at 30 Hz with a low accelerations less than 0.4 g. The maximum voltage and normalized power are 42 mV and 0.31  $\mu\text{W}/\text{g}^2$ , respectively. This cantilever was operated with the broad bandwidth from 3.4 to 11.1 Hz depending on the reduced stop distance from 1.7 to 0.7 mm under an acceleration of 0.3 g and the generated voltage and normalized power at the resonance frequency was reduced from 40 to 16 mV and from 17.8 to 2.8  $\text{nW}/\text{g}^2$ , respectively [61]. Moreover, in order to use in low vibrational environments under 48 Hz, they fabricated a cantilever-type stopper beside a MEMS cantilever energy harvester, which also generates the output voltage. Thus, both the stopper and the generator could concurrently produce the output voltage of 20 V and output power of 140 nW, respectively [62,63]. The achieving of wide bandwidth of the cantilever basically causes the low power generation, because of vibration compensation in the limited spacer technique and a phase mismatch between the cantilever arrays. To overcome these challenges, Hajati and Kim *et al.* developed an ultra-wide bandwidth piezoelectric energy harvester by exploiting a nonlinear stiffness of a double clamped MEMS resonator [52]. In this structure, the stretching strain is always applied to the beam, which causes uniform tensile stress, while the bending strain in the conventional cantilever structure is not uniform along the length and thickness of the elastic body. The tensile strain with the nonlinear stiffness provides passive feedback and results in this amplitude-stiffened Duffing mode resonance. The nonlinear resonator showed wide bandwidth exceeding 20% of the arithmetic center frequency and generated maximum power of  $\sim 45$   $\mu\text{W}$  at  $\sim 1.3$  kHz, which is much higher than other works that achieved wide bandwidth. The output performance of the MEMS piezoelectric vibration energy harvesters is summarized in Table 2.



**Table 2.** Comparison of the output performance of the microelectromechanical systems (MEMS) piezoelectric vibration energy harvesters.

Structure	Power Density ( $\mu\text{W}/\text{cm}^3$ )	Normalized Power ( $\mu\text{W}/\text{g}^2$ )	Frequency (Hz)	Ref.
Unimorph cantilever ( $d_{31}$ mode)	-	0.0061	89.4	[53]
Unimorph cantilever ( $d_{33}$ mode)	-	0.0335	89.4	[53]
Bimorph cantilever ( $d_{31}$ mode)	-	0.015	89.4	[53]
Bimorph cantilever ( $d_{33}$ mode)	-	0.035	89.4	[53]
Micro-cantilever using bulk PZT	28,856	11.6	520	[55]
Metal-based MEMS cantilever	98	15.4	89	[57]
Metal-based MEMS cantilever	15,453	89.0	112.4	[58]
Wideband cantilever	-	0.032–0.085	30–47	[59]
S-shape MEMS cantilever	-	0.31	27.4	[61]

#### 4. Flexible Piezoelectric Energy Harvesters

The PZT based materials have an outstanding piezoelectric coefficient and have been utilized for actuators, transducers, energy harvesters, *etc.* However, they tend to be easily brittle under a large strain and an applied force leading to several restrictions to be installed in flexible, wearable, and biocompatible electronic devices. The flexibility extends the feature of the piezoelectric materials and the application field for the emerging energy harvesting technology. Moreover, the flexibility of the piezoelectric energy harvesters enables obtaining large output power under large strain by the off-resonance vibration and deformation due to a remarkable endurance under the large strain. To acquire the flexibility in the piezoelectric ceramics, nano- and micro-structured materials, and thin films have been used with a polymer composite and a freestanding structure. The idea of an energy harvester using nanostructures was firstly reported by Zhong Lin Wang in 2006. He introduced the piezoelectricity in the ZnO having enough feasibility for the flexible piezoelectric energy harvesting [3]. Since he demonstrated the piezoelectric energy harvester using the ZnO nanostructures, significant studies have been reported about the piezoelectric nanogenerators, which used ZnO nanostructures. The PZT based nanostructured materials have significant larger piezoelectric coefficients than ZnO [64,65]. Nevertheless, only a limited number of studies have been reported about the flexible piezoelectric energy harvesting using the PZT based material, because of critical limitations to synthesizing nanostructures due to a complex composition and a higher crystallization temperature, which makes it to be not applicable with the flexible polymer materials. Herein, we focused on flexible piezoelectric energy harvesting devices using the PZT based flexible materials including nanotubes, nanorods, nanowires, nanofibers, nanocomposites, thin films, *etc.*

##### 4.1. Nanotubes

The PZT nanotubes have usually been synthesized by a template-assisted infiltration method using an anodic aluminum oxide (AAO). Xu *et al.* obtained electrical power from the PZT nanotubes, which have a high aspect ratio, by a template-assisted method. A pure perovskite phase with strong  $\langle 110 \rangle$  preferred crystallographic orientation was obtained by a heat treatment at 650 °C. The diameters of the nanotubes ranging from 190 to 210 nm were obtained, corresponding to diameter and height of the nanopores in the AAO template as shown in Figure 2a. The fabricated nanotubes were sandwiched between two Ag electrodes and the energy harvester generated the electrical power up to 496 mV when a stainless-steel nugget was dropped on the electrode (Figure 2b) [66]. The Korea Institute of Science and Technology (KIST) presented a composite generator using the PZT nanotubes. An AAO template-assisted method was used to fabricate the PZT nanotubes. The fabricated nanotubes had the length of 60  $\mu\text{m}$  and the diameter of 200 nm as shown in Figure 2c. For the flexibility of the device, polydimethylsiloxane (PDMS) elastomer was mixed with the fabricated nanotubes, and Pt coated polyimide (PI) films were attached on the bottom and top of the PZT–PDMS composite. The PZT–PDMS composite energy harvester generated about ~2 V and ~60 nA when the generator was bended and stretched (see Figure 2d) [67].

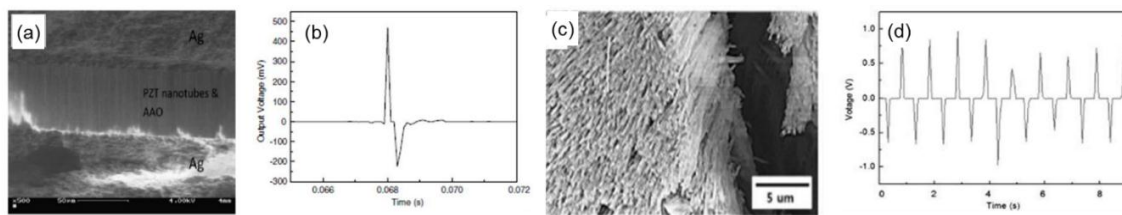


**Figure 2.** (a) Cross-sectional view of the device using PZT nanotubes [66]; (b) output voltage from the PZT nanotube arrays [66]; (c) PZT nanotubes [67]; (d) output performance of the PZT nanotube composite energy harvester [67].

#### 4.2. Nanorods and Nanowires

The PZT nanorods and nanowires have usually been synthesized by a hydrothermal method. Xu *et al.* demonstrated PZT nanowire arrays epitaxially grown on conductive substrates using a hydrothermal method [68]. Pt electrodes were used on both the top and bottom of the nanowires by electron beam evaporation. The entire structure was packaged with a soft epoxy polymer to ensure the robustness of the device and also isolate a possible moisture erosion to the nanowires. They assessed the output voltage and current from the fabricated device, connecting a rectifier circuit and a light emitting diode (LED), under various frequencies. The output voltage of the device reached around 1 V and the output current is over 200 nA under pressing motion. Using a capacitor with 22 μF, they successfully tested the LED lighting. In addition, through the test with a range of stimulating frequencies from 1 to 50 Hz, they expected the energy harvester can be configured to work under a relatively high frequency of ~50 kHz [68]. Wang *et al.* demonstrated a PZT nanowire textile energy harvester with generating ~6 V output voltage and ~45 nA output current during bending motion, which are large enough to power a liquid crystal display (LCD). They fabricated PZT nanowires by an electrospinning method. For the flexibility of the device, they aligned the parallel PZT nanowires on PDMS template as shown in Figure 3 [69]. Zhou *et al.* synthesized high quality single crystal PZT nanowires by a two-step hydrothermal method. Measured piezoelectric strain coupling coefficient of the PZT nanowire was 80 pm/V. To fabricate the flexible piezoelectric energy harvester, a nanocomposite cantilever was demonstrated with the PDMS elastomer. The harvester exhibited 2.4 μW/cm<sup>3</sup> of the maximum power density when it is vibrating [70].

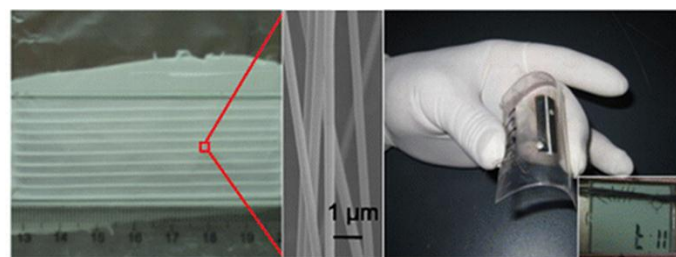


**Figure 3.** Nanocomposite generator using aligned PZT nanowires [69].

#### 4.3. Nanofibers

Piezoelectric nanofibers are promising structures to obtain the large strain and the flexibility with the high energy density. Qi *et al.* in Princeton University fabricated piezoelectric nanoribbons printed onto rubber for the flexible energy conversion. The PZT ribbons have a micrometer-scale width and nanometer scale thickness. To fabricate PZT ribbons, PZT films were grown on a (100)-cleaved MgO crystal substrate and post-annealed to obtain the perovskite crystal structure. The fabricated films were patterned into nano-thick ribbons and printed onto the PDMS via a dry transfer, as shown in Figure 4a. By this process, they overcame the limitation of the high temperature heat treatment for the

crystallization. In addition, they obtained the  $d_{33}$  value of 101 pm/V for the PZT ribbons after a poling. This value agrees well with the thin film data, which is understandable considering the relatively benign processing conditions for fabricating and transferring PZT ribbons [71]. They also represented a stretchable energy harvester using buckled PZT ribbons. The PZT ribbons were patterned on the MgO substrate and subsequently released from the substrate using the phosphoric acid. A slab of the PDMS was then elastically stretched and brought into a conformal contact with the ribbons. Finally, releasing the prestrain in the PDMS led to a compressive force on the PZT ribbons when the PDMS relaxed to zero strain, leading to a periodic de-adhesion and buckling as shown in Figure 4b. The measured  $d_{33}$  value was ~130 pm/V and the generated output current was about 100 pA [72]. Chen *et al.* utilized PZT nanofibers fabricated by an electrospinning method and deposited them onto the IDE of platinum fine wire arrays. The fabricated nanofibers have the diameter of 60 nm and were laterally aligned on electrodes for the longitudinal mode as shown in Figure 4c. The PZT nanofibers were polled by applying electric field across the electrodes, and then the silicon substrate was released for the flexibility of the device. In order to confirm the power generation from the device, the pressure was applied on the top surface. The output voltage was 0.6 V when applying a large load, and 1.63 V when applying the pressure with a finger [73].

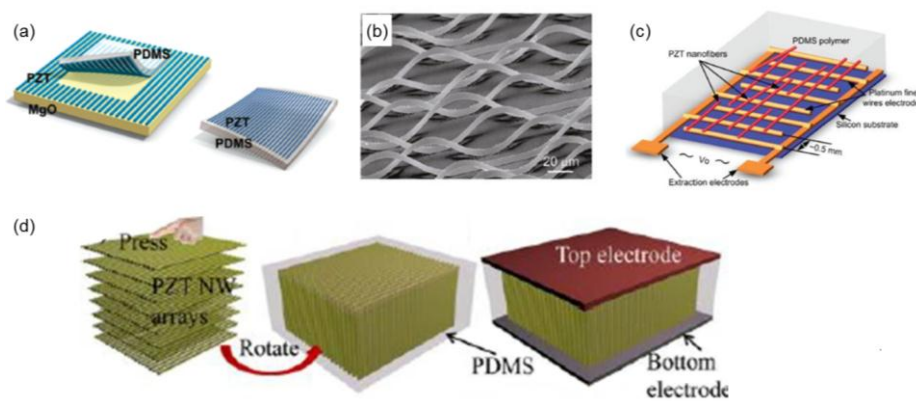


**Figure 4.** (a) Flexible PZT nanoribbons on the PDMS substrate [71]; (b) buckled PZT nanoribbons [72]; (c) energy harvester using aligned PZT nanofiber [73]; (d) nanogenerator using PZT nanofiber composite [75].

They also demonstrated a flexible acoustic emission sensor based on the PZT nanofiber composite membrane with a similar structure. The electrospinning method was used for the fabrication of the PZT nanofibers. The plastic substrate was used for the flexibility of the device. It was attached on the carbon fiber composite to measure an acoustic sensing performance. The device produced the output voltage of ~10 mV when the steel ball was dropped down to the carbon composite and up to ~100 mV when a steel bar hit the composite directly. They showed flexibility and self-powered sensing, and high sensitivity, which allows the possibility of monitoring structures by the curved surfaces or integrating into composite [74]. Gu *et al.* presented a flexible fiber nanogenerator, which enables turning on the light-emitting diodes. To fabricate vertically aligned PZT nanofiber arrays, the PZT nanofiber film was obtained first and it was stacked layer by layer to form multilayer films (see Figure 4d). PDMS was filled into the interspace of the films and nanofibers using a capillary force, and the multilayer film was gently pressed without damage of its structure. The electrodes were attached on the top and bottom surfaces of the fabricated device. In experimental results, the maximum output voltage was 209 V and the peak current was 53 μA. The output power was available for the self-powered system, such as sensor network [75].

#### 4.4. Nanoparticles

The PZT nanoparticles have been used as active materials in the composite piezoelectric energy harvesters. Park *et al.* reported the flexible and large-area nanocomposite generators (NCG) based on the PZT nanoparticles and carbon nanotubes. They used the PZT nanoparticles as an energy generation source to achieve the excellent output signal. The nanoparticles were mixed with the PDMS and CNTs in order to improve the flexibility and stretchability of the device. The CNTs, as dispersing agents, stress reinforcement, and conduction path, improved the output performance of the nanocomposite-based piezoelectric device. It produced the output voltage and current up to 10 V and 1.3  $\mu\text{A}$ , respectively. From a large-area NCG device with  $30 \times 30 \text{ cm}^2$ , they obtained the output voltage up to 100 V and the current signal up to 10  $\mu\text{A}$ . Using these devices, they turned on the LEDs and LCD screen [76]. Zhang *et al.* demonstrated a self-charging Li battery using a polyvinylidene fluoride (PVDF)-PZT nanoparticle composite separator (Figure 5). The piezoelectric potential from the separator could effectively drive the diffusion of Li ions. This device directly converted the mechanical energy into the electrochemical energy and stored it. The piezoelectric separator generated  $\sim 1 \text{ V}$  under periodic compressive stress of 10 N. The storage capacity of the PVDF-PZT based Li battery was  $\sim 0.010 \mu\text{Ah}$  in 240 s [77].

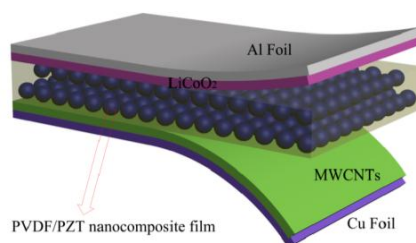


**Figure 5.** Self-charging Li battery using PVDF-PZT nanoparticle composite separator [77].

#### 4.5. Thin Films

Thin film materials also have remarkable potential for the flexible piezoelectric energy harvesting technology. However, the PZT thin film has many limitations to demonstrate the flexible devices, which need to be installed on flexible substrates because of their high crystallization temperature ( $<600^\circ\text{C}$ ). To overcome these challenges, Do *et al.* firstly reported a film transfer method using laser lift-off (LLO) process. They fabricated a transparent flexible piezoelectric energy harvester based on the PZT films by the LLO process as shown in Figure 6a. They synthesized the fully crystallized PZT thin film on the sapphire substrate. By the LLO process, the PZT thin film was transferred from the sapphire substrate to the flexible receptor substrate. In this process, an additional heat treatment was unnecessary to form the crystallized PZT film on the flexible substrate. Indium-tin-oxide (ITO) coated polyethylene terephthalate (PET) film was used as the electrodes and flexible substrate. Finally, they obtained the output signal generated from the device, resulting in the maximum output voltage of  $\sim 0.28 \text{ V}$  and output current of  $\sim 30 \text{ nA}$ . The average power density of the device with a total active area about  $1 \text{ cm} \times 1 \text{ cm}$  was approximately  $8.4 \text{ nW}/\text{cm}^2$  [78]. Park *et al.* also reported the flexible PZT energy harvester fabricated by the LLO process. They transferred the PZT thin films from the sapphire substrate to a plastic substrate and formed IDE patterns on the PZT thin film to fabricate the energy harvester. The energy harvester generated  $\sim 200 \text{ V}$  of output voltage and  $150 \mu\text{A}/\text{cm}^2$  of current, and turned on over 100 blue LEDs without any external electric source [79]. Using this technique, they also fabricated a self-powered flexible embedded LED system [80] and a nanosensor for biomedical applications [81]. Chun *et al.* demonstrated a highly-stretchable composite nanogenerator using a hemisphere PZT thin film [82]. The hemisphere PZT thin film was produced using a polystyrene (PS) sphere template. To fabricate the composite energy harvester, PDMS was filled into the hemisphere PZT thin film and the substrate was removed by the lift-off method as shown in Figure 6b. The energy

harvester generated 4 V of the output voltage and  $0.13 \mu\text{A}/\text{cm}^2$  of the current during a periodic bending motion. The output performance of the flexible piezoelectric energy harvesters is summarized in Table 3.

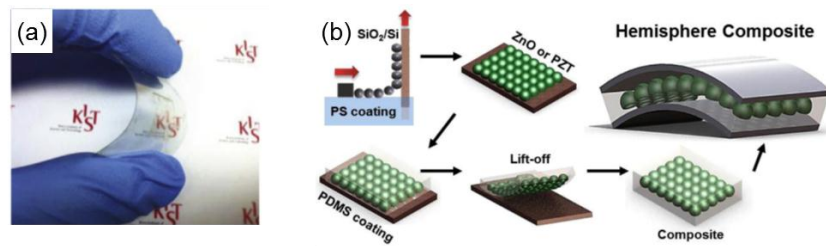


**Figure 6.** (a) Transparent flexible piezoelectric energy harvester based on PZT films by LLO process [78]; (b) highly-stretchable composite nanogenerator using hemisphere PZT thin film [82].

**Table 3.** Comparison of the output performance of flexible piezoelectric energy harvesters.

Structure	Max. Voltage	Max. Current	Max. Power	Ref.
Freestanding PZT nanotube	0.495 V	-	-	[66]
PZT nanotube composite	2 V	60 nA	-	[67]
PZT nanorod arrays	1 V	200 nA	-	[68]
PZT nanowire textile	6 V	45 nA	-	[69]
PZT nanowire composite	4 V	88 nA	$2.4 \mu\text{W}/\text{cm}^3$	[70]
Buckled PZT nano-ribbons	-	100 pA	-	[72]
PZT nano fibers	1.63 V	-	$0.03 \mu\text{W}$	[73]
Vertically aligned PZT nanofiber arrays	209 V	53 $\mu\text{A}$	$4.9 \text{ mW}/\text{cm}^2$	[75]
PZT nanoparticle composite	10 V	1.3 $\mu\text{A}$	13 $\mu\text{W}$	[76]
Transparent PZT thin film harvester (sandwich structure)	0.28 V	30 nA	$8.4 \text{ nW}/\text{cm}^2$	[78]
PZT thin film harvester (planar structure)	200 V	$150 \mu\text{A}/\text{cm}^2$	$30 \text{ mW}/\text{cm}^2$	[79]
Hemisphere PZT thin film composite	4 V	$0.13 \mu\text{A}/\text{cm}^2$	$0.52 \mu\text{W}/\text{cm}^2$	[82]

## 5. Conclusions

PZT based energy harvesting technologies reported in the last few years are summarized in this paper. The following three focuses were derived from this study. First, the PZT based bulk piezoelectric energy harvesters have been suggested for self-powered systems. For the practical application, the resonance frequency has been tuned to the low frequency in the cantilever type piezoelectric energy harvesters by controlling the structural parameters. Unique designs of the bulk type energy harvesters provided a higher efficiency in certain environmental conditions including resonance vibration, off-resonance, impact, *etc.* Second, various designs of the MEMS piezoelectric energy harvesters have usually been based on the cantilever structure, and have been studied to control the resonance frequencies and achieve wide bandwidth for practical applications. Finally, flexible piezoelectric energy harvesters using nano-materials, which allow flexibility for the piezoelectric materials, enabled the off-resonance operation of the piezoelectric energy harvester with the remarkable strength under the large strain. However, although the larger strain is induced on the flexible energy harvesters, the output power is still lower than the bulk and MEMS piezoelectric energy harvesters that operated at resonance frequency. The off-resonance operation and very lower packing density of the active piezoelectric materials of the flexible energy harvesters resulted in a low output power. Nevertheless, from a different point of view, the flexible piezoelectric energy harvesters are very attractive in a random vibration environment, such as the wind, water flow, human movement, *etc.*

From this paper, here, we anticipate that the bulk and MEMS energy harvesters should be designed to determine the resonance frequency for an exact application because the vibration sources that are vibrating in a certain frequency regularly are the only optimum sources for these two techniques.



Therefore, achieving wide bandwidth is the most reasonable way for them to be used in practical applications. For enhancing the performance of the flexible piezoelectric energy harvesting technology, the packing density of the active piezoelectric materials should be increased while maintaining flexibility. Moreover, the specific units of the output voltage, current, and power need to be uniform and standardized for the piezoelectric energy harvesting technology except for cantilever type harvesters.

**Acknowledgments:** This work was supported by the Converging Research Center Program by the Ministry of Education, Science and Technology (2010K000979), Korea.

**Author Contributions:** Min Gyu Kang and Woo-Suk Jung built and wrote the majority of the manuscript text. This review paper was directed by Chong-Yun Kang and Seok-Jin Yoon. All authors reviewed the manuscript.

**Conflicts of Interest:** The authors declare no conflict of interest.

## References

1. Park, S.E.; Shrout, T.R. Characteristics of relaxor-based piezoelectric single crystals for ultrasonic transducers. *IEEE Trans. Ultrason. Ferroelectr. Freq. Control* **1997**, *44*, 1140–1147. [[CrossRef](#)]
2. Dubois, M.A.; Muralt, P. Properties of aluminum nitride thin films for piezoelectric transducers and microwave filter applications. *Appl. Phys. Lett.* **1999**, *74*, 3032–3034. [[CrossRef](#)]
3. Wang, X.D.; Zhou, J.; Song, J.H.; Liu, J.; Xu, N.S.; Wang, Z.L. Piezoelectric field effect transistor and nanoforce sensor based on a single ZnO nanowire. *Nano Lett.* **2006**, *6*, 2768–2772. [[CrossRef](#)] [[PubMed](#)]
4. Giurgiutiu, V. *Structural Health Monitoring with Piezoelectric Wafer Active Sensors*, 2nd ed.; Academic Press: Cambridge, MA, USA, 2014; pp. 1–1012.
5. Ihn, J.B.; Chang, F.K. Detection and monitoring of hidden fatigue crack growth using a built-in piezoelectric sensor/actuator network: I. Diagnostics. *Smart Mater. Struct.* **2004**, *13*, 609–620. [[CrossRef](#)]
6. Uchino, K. Materials issues in design and performance of piezoelectric actuators: An overview. *Acta Mater.* **1998**, *46*, 3745–3753. [[CrossRef](#)]
7. Wang, Q.M.; Zhang, Q.M.; Xu, B.M.; Liu, R.B.; Cross, L.E. Nonlinear piezoelectric behavior of ceramic bending mode actuators under strong electric fields. *J. Appl. Phys.* **1999**, *86*, 3352–3360. [[CrossRef](#)]
8. Chu, S.Y.; Chen, T.Y.; Tsai, I.T.; Water, W. Doping effects of Nb additives on the piezoelectric and dielectric properties of PZT ceramics and its application on saw device. *Sens. Actuators A Phys.* **2004**, *113*, 198–203. [[CrossRef](#)]
9. Tang, I.T.; Chen, H.J.; Hwang, W.C.; Wang, Y.C.; Hwang, M.P.; Wang, Y.H. Applications of piezoelectric ZnO film deposited on diamond-like carbon coated onto Si substrate under fabricated diamond saw filter. *J. Cryst. Growth* **2004**, *262*, 461–466. [[CrossRef](#)]
10. Kim, H.S.; Kim, J.H.; Kim, J. A review of piezoelectric energy harvesting based on vibration. *Int. J. Precis. Eng. Man.* **2011**, *12*, 1129–1141. [[CrossRef](#)]
11. Beeby, S.P.; Tudor, M.J.; White, N.M. Energy harvesting vibration sources for microsystems applications. *Meas. Sci. Technol.* **2006**, *17*, R175–R195. [[CrossRef](#)]
12. Uchino, K. *Ferroelectric Devices*, 2nd ed.; CRC Press: Boca Raton, FL, USA, 2010; pp. 161–169.
13. Ouyang, J.; Ramesh, R.; Roytburd, A.L. Intrinsic effective piezoelectric coefficient  $e_{31,f}$  for ferroelectric thin films. *Appl. Phys. Lett.* **2005**, *86*, 152901. [[CrossRef](#)]
14. Maria, J.P.; Shepard, J.F.; Troler-McKinstry, S.; Watkins, T.R.; Payzant, A.E. Characterization of the piezoelectric properties of  $\text{Pb}_{0.98}\text{Ba}_{0.02}(\text{Mg}_{1/3}\text{Nb}_{2/3})\text{O}_3$ - $\text{PbTiO}_3$  epitaxial thin films. *Int. J. Appl. Ceram. Technol.* **2005**, *2*, 51–58. [[CrossRef](#)]
15. Shrout, T.R.; Zhang, S.J. Lead-free piezoelectric ceramics: Alternatives for PZT? *J. Electroceram.* **2007**, *19*, 113–126. [[CrossRef](#)]
16. Tao, H.; Wu, J.G.; Xiao, D.Q.; Zhu, J.G.; Wang, X.J.; Lou, X.J. High strain in (K,Na)NbO<sub>3</sub>-based lead-free piezoceramics. *ACS Appl. Mater. Inter.* **2014**, *6*, 20358–20364. [[CrossRef](#)] [[PubMed](#)]
17. Rubio-Marcos, F.; Ochoa, P.; Fernandez, J.F. Sintering and properties of lead-free (K,Na,Li)(Nb,Ta,Sb)O<sub>3</sub> ceramics. *J. Eur. Ceram. Soc.* **2007**, *27*, 4125–4129. [[CrossRef](#)]
18. Zhang, M.; Yang, J.; Si, C.W.; Han, G.W.; Zhao, Y.M.; Ning, J. Research on the piezoelectric properties of AlN thin films for MEMS applications. *Micromachines* **2015**, *6*, 1236–1248. [[CrossRef](#)]

19. Zhao, M.H.; Wang, Z.L.; Mao, S.X. Piezoelectric characterization of individual zinc oxide nanobelt probed by piezoresponse force microscope. *Nano Lett.* **2004**, *4*, 587–590. [[CrossRef](#)]
20. Wang, Z.L.; Song, J.H. Piezoelectric nanogenerators based on zinc oxide nanowire arrays. *Science* **2006**, *312*, 242–246. [[CrossRef](#)] [[PubMed](#)]
21. Kumar, B.; Kim, S.W. Energy harvesting based on semiconducting piezoelectric ZnO nanostructures. *Nano Energy* **2012**, *1*, 342–355. [[CrossRef](#)]
22. Kim, K.B.; Kim, C.I.; Jeong, Y.H.; Lee, Y.J.; Cho, J.H.; Paik, J.H.; Nahm, S. Performance of unimorph cantilever generator using Cr/Nb doped  $\text{Pb}(\text{Zr}_{0.54}\text{Ti}_{0.46})\text{O}_3$  thick film for energy harvesting device applications. *J. Eur. Ceram. Soc.* **2013**, *33*, 305–311. [[CrossRef](#)]
23. Choi, C.H.; Seo, I.T.; Song, D.; Jang, M.S.; Kim, B.Y.; Nahm, S.; Sung, T.H.; Song, H.C. Relation between piezoelectric properties of ceramics and output power density of energy harvester. *J. Eur. Ceram. Soc.* **2013**, *33*, 1343–1347. [[CrossRef](#)]
24. Kim, S.B.; Park, J.H.; Ahn, H.; Liu, D.; Kim, D.J. Temperature effects on output power of piezoelectric vibration energy harvesters. *Microelectron. J.* **2011**, *42*, 988–991. [[CrossRef](#)]
25. Song, H.C.; Kang, C.Y.; Yoon, S.J.; Jeong, D.Y. Engineered domain configuration and piezoelectric energy harvesting in  $0.7\text{Pb}(\text{Mg}_{1/3}\text{Nb}_{2/3})\text{O}_3$ – $0.3\text{PbTiO}_3$  single crystals. *Metals Mater. Int.* **2012**, *18*, 499–503. [[CrossRef](#)]
26. Karami, M.A.; Bilgen, O.; Inman, D.J.; Friswell, M.I. Experimental and analytical parametric study of single-crystal unimorph beams for vibration energy harvesting. *IEEE Trans. Ultrason. Ferroelectr. Freq. Control* **2011**, *58*, 1508–1520. [[CrossRef](#)] [[PubMed](#)]
27. Priya, S.; Inman, D.J. *Energy Harvesting Technologies*; Springer: New York, NY, USA, 2009; p. 517.
28. Berdy, D.F.; Srisungsitthisunti, P.; Jung, B.; Xu, X.F.; Rhoads, J.F.; Peroulis, D. Low-frequency meandering piezoelectric vibration energy harvester. *IEEE Trans. Ultrason. Ferroelectr. Freq. Control* **2012**, *59*, 846–858. [[CrossRef](#)] [[PubMed](#)]
29. Shindo, Y.; Narita, F. Dynamic bending/torsion and output power of s-shaped piezoelectric energy harvesters. *Int. J. Mech. Mater. Des.* **2014**, *10*, 305–311. [[CrossRef](#)]
30. Sobocinski, M.; Leinonen, M.; Juuti, J.; Jantunen, H. Monomorph piezoelectric wideband energy harvester integrated into LTCC. *J. Eur. Ceram. Soc.* **2011**, *31*, 789–794. [[CrossRef](#)]
31. Park, J.C.; Park, J.Y. Asymmetric PZT bimorph cantilever for multi-dimensional ambient vibration harvesting. *Ceram. Int.* **2013**, *39*, S653–S657. [[CrossRef](#)]
32. Hashimoto, S.; Zhang, Y.; Nagai, N.; Fujikura, Y.; Takahashi, J.; Kumagai, S.; Kasai, M.; Suto, K.; Okada, H.; Jiang, W. Multi-mode and multi-axis vibration power generation effective for vehicles. In Proceedings of the 2013 IEEE International Symposium on Industrial Electronics, Taipei, Taiwan, 28–31 May 2013.
33. Ethem Erkan Aktakka, K.N. Three-axis piezoelectric vibration energy harvester. In Proceedings of 28th IEEE International Conference on Micro Electro Mechanical Systems, Estoril, Portugal, 18–22 January 2015.
34. Khameneifar, F.; Arzanpour, S.; Moallem, M. A piezoelectric energy harvester for rotary motion applications: Design and experiments. *IEEE ASME Trans. Mechatron.* **2013**, *18*, 1527–1534. [[CrossRef](#)]
35. Yang, Y.; Shen, Q.L.; Jin, J.M.; Wang, Y.P.; Qian, W.J.; Yuan, D.W. Rotational piezoelectric wind energy harvesting using impact-induced resonance. *Appl. Phys. Lett.* **2014**, *105*, 053901. [[CrossRef](#)]
36. Pozzi, M.; Aung, M.S.H.; Zhu, M.L.; Jones, R.K.; Goulermas, J.Y. The pizzicato knee-joint energy harvester: Characterization with biomechanical data and the effect of backpack load. *Smart Mater. Struct.* **2012**, *21*, 076023. [[CrossRef](#)]
37. Li, B.; You, J.H.; Kim, Y.J. Low frequency acoustic energy harvesting using PZT piezoelectric plates in a straight tube resonator. *Smart Mater. Struct.* **2013**, *22*, 055013. [[CrossRef](#)]
38. Palosaari, J.; Leinonen, M.; Hannu, J.; Juuti, J.; Jantunen, H. Energy harvesting with a cymbal type piezoelectric transducer from low frequency compression. *J. Electroceram.* **2012**, *28*, 214–219. [[CrossRef](#)]
39. Chen, X.R.; Yang, T.Q.; Wang, W.; Yao, X. Vibration energy harvesting with a clamped piezoelectric circular diaphragm. *Ceram. Int.* **2012**, *38*, S271–S274. [[CrossRef](#)]
40. Zhao, S.; Erturk, A. Deterministic and band-limited stochastic energy harvesting from uniaxial excitation of a multilayer piezoelectric stack. *Sens. Actuators. A Phys.* **2014**, *214*, 58–65. [[CrossRef](#)]
41. Xu, T.B.; Siochi, E.J.; Kang, J.H.; Zuo, L.; Zhou, W.L.; Tang, X.D.; Jiang, X.N. Energy harvesting using a PZT ceramic multilayer stack. *Smart Mater. Struct.* **2013**, *22*, 065015. [[CrossRef](#)]

42. Makki, N.; Pop-Iliev, R. Battery- and wire-less tire pressure measurement systems (TPMS) sensor. *Microsyst. Technol.* **2012**, *18*, 1201–1212. [[CrossRef](#)]
43. Roundy, S.; Wright, P.K. A piezoelectric vibration based generator for wireless electronics. *Smart Mater. Struct.* **2004**, *13*, 1131–1142. [[CrossRef](#)]
44. Renaud, M.; Karakaya, K.; Sterken, T.; Fiorini, P.; Van Hoof, C.; Puers, R. Fabrication, modelling and characterization of mems piezoelectric vibration harvesters. *Sens. Actuators A Phys.* **2008**, *145*, 380–386. [[CrossRef](#)]
45. Shen, D.; Park, J.H.; Ajitsaria, J.; Choe, S.Y.; Wickle, H.C.; Kim, D.J. The design, fabrication and evaluation of a MEMS PZT cantilever with an integrated Si proof mass for vibration energy harvesting. *J. Micromech. Microeng.* **2008**, *18*, 055017. [[CrossRef](#)]
46. Janphuang, P.; Lockhart, R.; Uffer, N.; Briand, D.; de Rooij, N.F. Vibrational piezoelectric energy harvesters based on thinned bulk PZT sheets fabricated at the wafer level. *Sens. Actuators A Phys.* **2014**, *210*, 1–9. [[CrossRef](#)]
47. Cui, Y.; Zhang, Q.Y.; Yao, M.L.; Dong, W.J.; Gao, S.Q. Vibration piezoelectric energy harvester with multi-beam. *AIP Adv.* **2015**, *5*, 041332. [[CrossRef](#)]
48. Deng, L.C.; Wen, Z.Y.; Zhao, X.Q.; Yuan, C.W.; Luo, G.X.; Mo, J.K. High voltage output MEMS vibration energy harvester in  $d_{31}$  mode with PZT thin film. *J. Microelectromech. Syst.* **2014**, *23*, 855–861. [[CrossRef](#)]
49. Liu, H.C.; Zhang, S.S.; Kobayashi, T.; Chen, T.; Lee, C. Flow sensing and energy harvesting characteristics of a wind-driven piezoelectric  $\text{Pb}(\text{Zr}_{0.52}\text{Ti}_{0.48})\text{O}_3$  microcantilever. *Micro Nano Lett.* **2014**, *9*, 286–289. [[CrossRef](#)]
50. Kim, M.; Hwang, B.; Min, N.K.; Jeong, J.; Kwon, K.H.; Park, K.B. Design and fabrication of a PZT cantilever for low frequency vibration energy harvesting. *J. Nanosci. Nanotechnol.* **2011**, *11*, 6510–6513. [[CrossRef](#)] [[PubMed](#)]
51. Kuehne, I.; Schreiter, M.; Seidel, J.; Seidel, H.; Frey, A. A novel MEMS design of a piezoelectric generator for fluid-actuated energy conversion. *Proc. SPIE* **2011**, *8066*, 806617.
52. Hajati, A.; Kim, S.G. Ultra-wide bandwidth piezoelectric energy harvesting. *Appl. Phys. Lett.* **2011**, *99*, 083105. [[CrossRef](#)]
53. Kim, M.; Hwang, B.; Jeong, J.; Min, N.K.; Kwon, K.H. Micromachining of a bimorph  $\text{Pb}(\text{Zr,Ti})\text{O}_3$  (PZT) cantilever using a micro-electromechanical systems (MEMS) process for energy harvesting application. *J. Nanosci. Nanotechnol.* **2012**, *12*, 6011–6015. [[PubMed](#)]
54. Kim, S.B.; Park, H.; Kim, S.H.; Wickle, H.C.; Park, J.H.; Kim, D.J. Comparison of MEMS PZT cantilevers based on  $d(31)$  and  $d(33)$  modes for vibration energy harvesting. *J. Microelectromech. Syst.* **2013**, *22*, 26–33. [[CrossRef](#)]
55. Tang, G.; Liu, J.Q.; Yang, B.; Luo, J.B.; Liu, H.S.; Li, Y.G.; Yang, C.S.; He, D.N.; Dao, V.D.; Tanaka, K.; et al. Fabrication and analysis of high-performance piezoelectric MEMS generators. *J. Micromech. Microeng.* **2012**, *22*, 065017. [[CrossRef](#)]
56. Tang, G.; Liu, J.Q.; Liu, H.S.; Li, Y.G.; Yang, C.S.; He, D.N.; DzungDao, V.; Tanaka, K.; Sugiyama, S. Piezoelectric MEMS generator based on the bulk PZT/silicon wafer bonding technique. *Phys. Status Solidi A* **2011**, *208*, 2913–2919. [[CrossRef](#)]
57. Wang, Q.; Cao, Z.P.; Kuwano, H. Metal-based piezoelectric energy harvesters by direct deposition of PZT thick films on stainless steel. *Micro Nano Lett.* **2012**, *7*, 1158–1161. [[CrossRef](#)]
58. Lin, S.C.; Wu, W.J. Piezoelectric micro energy harvesters based on stainless-steel substrates. *Smart Mater. Struct.* **2013**, *22*, 045016. [[CrossRef](#)]
59. Liu, H.C.; Tay, C.J.; Quan, C.G.; Kobayashi, T.; Lee, C. Piezoelectric MEMS energy harvester for low-frequency vibrations with wideband operation range and steadily increased output power. *J. Microelectromech. Syst.* **2011**, *20*, 1131–1142. [[CrossRef](#)]
60. Liu, H.C.; Quan, C.G.; Tay, C.J.; Kobayashi, T.; Lee, C. A MEMS-based piezoelectric cantilever patterned with PZT thin film array for harvesting energy from low frequency vibrations. *Phys. Proc.* **2011**, *19*, 129–133. [[CrossRef](#)]
61. Liu, H.C.; Lee, C.; Kobayashi, T.; Tay, C.J.; Quan, C.G. A new S-shaped MEMS PZT cantilever for energy harvesting from low frequency vibrations below 30 Hz. *Microsyst. Technol.* **2012**, *18*, 497–506. [[CrossRef](#)]
62. Liu, H.C.; Zhang, S.S.; Kathiresan, R.; Kobayashi, T.; Lee, C. Development of piezoelectric microcantilever flow sensor with wind-driven energy harvesting capability. *Appl. Phys. Lett.* **2012**, *100*, 223905. [[CrossRef](#)]

63. Liu, H.C.; Lee, C.; Kobayashi, T.; Tay, C.J.; Quan, C.G. A MEMS-based wideband piezoelectric energy harvester system using mechanical stoppers. In Proceedings of the 2011 IEEE International Electron Devices Meeting, Washington, DC, USA, 5–7 December 2011.
64. Xu, G.; Ren, Z.H.; Du, P.Y.; Weng, W.J.; Shen, G.; Han, G.R. Polymer-assisted hydrothermal synthesis of single-crystalline tetragonal perovskite  $\text{PbZr}_{0.52}\text{Ti}_{0.48}\text{O}_3$  nanowires. *Adv. Mater.* **2005**, *17*, 907–910. [[CrossRef](#)]
65. Zhang, X.Y.; Zhao, X.; Lai, C.W.; Wang, J.; Tang, X.G.; Dai, J.Y. Synthesis and piezoresponse of highly ordered  $\text{Pb}(\text{Zr}_{0.53}\text{Ti}_{0.47})\text{O}_3$  nanowire arrays. *Appl. Phys. Lett.* **2004**, *85*, 4190–4192. [[CrossRef](#)]
66. Xu, S.Y.; Shi, Y. Power generation from piezoelectric lead zirconate titanate nanotubes. *J. Phys. D Appl. Phys.* **2009**, *42*, 085301. [[CrossRef](#)]
67. Jung, W.S.; Do, Y.H.; Kang, M.G.; Kang, C.Y. Energy harvester using PZT nanotubes fabricated by template-assisted method. *Curr. Appl. Phys.* **2013**, *13*, S131–S134. [[CrossRef](#)]
68. Xu, S.; Hansen, B.J.; Wang, Z.L. Piezoelectric-nanowire-enabled power source for driving wireless microelectronics. *Nat. Commun.* **2010**, *1*, 1098. [[CrossRef](#)] [[PubMed](#)]
69. Wu, W.W.; Bai, S.; Yuan, M.M.; Qin, Y.; Wang, Z.L.; Jing, T. Lead zirconate titanate nanowire textile nanogenerator for wearable energy-harvesting and self-powered devices. *ACS Nano* **2012**, *6*, 6231–6235. [[CrossRef](#)] [[PubMed](#)]
70. Zhou, Z.; Tang, H.X.; Sodano, H.A. Scalable synthesis of morphotropic phase boundary lead zirconium titanate nanowires for energy harvesting. *Adv. Mater.* **2014**, *26*, 7547–7554. [[CrossRef](#)] [[PubMed](#)]
71. Qi, Y.; Jafferis, N.T.; Lyons, K.; Lee, C.M.; Ahmad, H.; McAlpine, M.C. Piezoelectric ribbons printed onto rubber for flexible energy conversion. *Nano Lett.* **2010**, *10*, 524–528. [[CrossRef](#)] [[PubMed](#)]
72. Qi, Y.; Kim, J.; Nguyen, T.D.; Lisko, B.; Purohit, P.K.; McAlpine, M.C. Enhanced piezoelectricity and stretchability in energy harvesting devices fabricated from buckled PZT ribbons. *Nano Lett.* **2011**, *11*, 1331–1336. [[CrossRef](#)] [[PubMed](#)]
73. Chen, X.; Xu, S.Y.; Yao, N.; Shi, Y. 1.6 V nanogenerator for mechanical energy harvesting using PZT nanofibers. *Nano Lett.* **2010**, *10*, 2133–2137. [[CrossRef](#)] [[PubMed](#)]
74. Chen, X.; Guo, S.; Li, J.; Zhang, G.T.; Lu, M.; Shi, Y. Flexible piezoelectric nanofiber composite membranes as high performance acoustic emission sensors. *Sens. Actuators A Phys.* **2013**, *199*, 372–378. [[CrossRef](#)]
75. Gu, L.; Cui, N.Y.; Cheng, L.; Xu, Q.; Bai, S.; Yuan, M.M.; Wu, W.W.; Liu, J.M.; Zhao, Y.; Ma, F.; *et al.* Flexible fiber nanogenerator with 209 V output voltage directly powers a light-emitting diode. *Nano Lett.* **2013**, *13*, 91–94. [[CrossRef](#)] [[PubMed](#)]
76. Park, K.I.; Jeong, C.K.; Ryu, J.; Hwang, G.T.; Lee, K.J. Flexible and large-area nanocomposite generators based on lead zirconate titanate particles and carbon nanotubes. *Adv. Energy Mater.* **2013**, *3*, 1539–1544. [[CrossRef](#)]
77. Zhang, Y.; Zhang, Y.J.; Xue, X.Y.; Cui, C.X.; He, B.; Nie, Y.X.; Deng, P.; Wang, Z.L. PVDF-PZT nanocomposite film based self-charging power cell. *Nanotechnology* **2014**, *25*, 105401. [[CrossRef](#)] [[PubMed](#)]
78. Do, Y.H.; Jung, W.S.; Kang, M.G.; Kang, C.Y.; Yoon, S.J. Preparation on transparent flexible piezoelectric energy harvester based on PZT films by laser lift-off process. *Sens. Actuators A Phys.* **2013**, *200*, 51–55. [[CrossRef](#)]
79. Park, K.I.; Son, J.H.; Hwang, G.T.; Jeong, C.K.; Ryu, J.; Koo, M.; Choi, I.; Lee, S.H.; Byun, M.; Wang, Z.L.; *et al.* Highly-efficient, flexible piezoelectric PZT thin film nanogenerator on plastic substrates. *Adv. Mater.* **2014**, *26*, 2514–2520. [[CrossRef](#)] [[PubMed](#)]
80. Jeong, C.K.; Park, K.I.; Son, J.H.; Hwang, G.T.; Lee, S.H.; Park, D.Y.; Lee, H.E.; Lee, H.K.; Byun, M.; Lee, K.J. Self-powered fully-flexible light-emitting system enabled by flexible energy harvester. *Energ. Environ. Sci.* **2014**, *7*, 4035–4043. [[CrossRef](#)]
81. Hwang, G.T.; Byun, M.; Jeong, C.K.; Lee, K.J. Flexible piezoelectric thin-film energy harvesters and nanosensors for biomedical applications. *Adv. Healthc. Mater.* **2015**, *4*, 646–658. [[CrossRef](#)] [[PubMed](#)]
82. Chun, J.; Kang, N.R.; Kim, J.Y.; Noh, M.S.; Kang, C.Y.; Choi, D.; Kim, S.W.; Wang, Z.L.; Baik, J.M. Highly anisotropic power generation in piezoelectric hemispheres composed stretchable composite film for self-powered motion sensor. *Nano Energy* **2015**, *11*, 1–10. [[CrossRef](#)]

